THE ANALYST
FULL PAPER
www.rsc.org/analyst

On-line monitoring of electroosmotic flow for capillary electrophoretic separations

Jason L. Pittman,[a] Kimberley F. Schrum[b] and S. Douglass Gilman*[a]

[a] *Department of Chemistry, University of Tennessee, Knoxville, TN 37996-1600, USA. E-mail: sdgilman@utk.edu; Fax: (865) 974-3454*
[b] *Department of Chemistry, Whittier College, Whittier, CA 90608, USA*

Received 12th April 2001, Accepted 20th June 2001
First published as an Advance Article on the web 23rd July 2001

A recently developed technique for monitoring electroosmotic flow (EOF) in capillary electrophoresis by periodic photobleaching of a neutral fluorophore added to the running buffer has been further characterized and optimized and then applied to monitoring EOF during a typical capillary electrophoresis separation. The concentration of neutral fluorophore (rhodamine B) added to the running buffer for monitoring EOF has been decreased by one order of magnitude. The rate at which EOF can be measured has been increased from 0.2 to 1.0 Hz by decreasing the distance between the bleaching beam and the laser-induced fluorescence detector from 6.13 to 0.635 mm. The precision of the measured EOF ranges from 0.2 to 1.8%. Under typical experimental conditions, the dynamic range for flow measurements is 0.066 to 0.73 cm s^{-1}. Experimental factors affecting precision, signal-to-noise (S/N) ratio and dynamic range for EOF monitoring have been examined. This technique has been applied to measure EOF during a separation of phenolic acids with analyte detection by UV/VIS absorbance. The EOF monitoring method has been shown not to interfere with UV/VIS absorbance detection of analytes.

1 Introduction

Precision limits the wide acceptance of capillary electrophoresis (CE) in laboratories required to submit results to regulatory agencies.[1–3] The precision of retention times, peak areas and peak heights obtained with CE are typically an order of magnitude poorer than that obtained with HPLC.[2] Fluctuations in electroosmotic flow (EOF) often result in variations of retention times of 3–5%, hindering the ability to identify and quantify analytes.[1–3] Therefore, it is important to measure and understand EOF for CE separations.

Typically, EOF is measured by injecting a neutral marker with the sample.[4,5] The migration time of the neutral marker provides a single, average value of EOF. However, this method has two significant shortcomings. Fluctuations of EOF that take place on a time scale faster than the neutral marker's elution time cannot be resolved. Also, the average EOF value does not include changes that occur after detection of the neutral marker although charged analytes may be detected after this time. Therefore, it is desirable to monitor EOF over an entire separation with time resolution faster than the total separation time. This will enable measurement and study of EOF fluctuations and correction of CE data for variations in EOF.

A variety of approaches have been used to continuously monitor or image EOF in capillaries.[6–15] Most imaging studies have focussed on observing flow profiles of electrokinetic and pressure-driven flow in capillaries, but these techniques have not been used for continuous monitoring of EOF.[7,8,11–14] Only two reported techniques for continuous EOF monitoring provide time resolution of less than 10 s and measurement precision of better than 1%.[9,15] Zare and coworkers monitored EOF by measuring the dilution of a fluorophore stream mixed with the effluent from the separation capillary.[9] The concentration of the fluorophore downstream from the post-column mixing device was inversely proportional to the rate of EOF in the separation capillary. These measurements were made with a time resolution of $\simeq$ 1 s and a precision of better than 1%.[9] Schrum *et al*. reported a method for EOF monitoring based on periodic photobleaching and laser-induced fluorescence (LIF) detection of a neutral fluorophore added to the running buffer at nanomolar concentrations.[15] Electroosmotic flow was measured by determining the time for a photobleached zone generated on-column to migrate $\simeq$ 6 mm to a downstream LIF detector. This measurement was repeated for EOF monitoring, providing a time resolution of 5.0 s and a precision of 0.7% or better.

Two related approaches for measuring flow in capillaries have been demonstrated.[16,17] Sugarman and Prud'homme measured flow by monitoring the change of fluorescence signal for a single-point LIF detector at high laser power.[16] They showed that fluorescein fluorescence under these conditions was dependent on the rate of Poiseuille flow in a 25 μm id capillary for flow rates of the order of 100 nL min^{-1}. StClaire and Hayes used a heating coil to periodically raise the temperature of a solution zone in a capillary.[17] This heated zone was detected 9 mm downstream based on the resulting change in refractive index. The migration time of the heated zone was used to determine the rate of Poiseuille flow in a 184 μm id capillary.[17] The time resolution and precision obtained were not reported for either of these methods.

The goals of the research presented in this paper are to improve the performance of the EOF monitoring technique reported by Schrum *et al*.[15] and to demonstrate the application of this technique to a typical CE separation with UV/VIS absorbance detection. The instrument has been modified to improve the time resolution of EOF monitoring. This is important for studying rapid fluctuations in EOF and for applying the technique to fast CE separations.[18–20] The concentration of the neutral fluorescent dye added to the running buffer for EOF monitoring has been reduced, which will decrease the potential for interference of the dye with analyte detection. We demonstrate that this method for EOF monitoring can be used with a CE separation and does not interfere with simultaneous detection of analytes using a separate UV/VIS absorbance detector.

 DOI: 10.1039/b103316f

2 Experimental

2.1 Materials

Laser grade rhodamine B, syringic acid, 4-hydroxy-3-methoxybenzoic acid, *p*-hydroxycinnamic acid, 3,4-dihydroxybenzoic acid, 3,4-dihydroxycinnamic acid, and gallic acid were obtained from Acros (Pittsburgh, PA). Mesityl oxide was purchased from Aldrich (Milwaukee, WI). Dimethyl sulfoxide (DMSO) was obtained from Mallinckrodt (Phillipsburg, NJ). Boric acid, sodium bicarbonate and HPLC grade methanol were purchased from Fisher Scientific (Pittsburgh, PA). All solutions were prepared in doubly distilled water.

2.2 EOF monitoring instrument

The previously reported instrument for EOF monitoring was modified to simplify monitoring of the opening of the computer-controlled shutter.[15] A single fiber optic (147.0 μm core; 164.0 μm cladding; Polymicro Technologies, Phoenix, AZ) was used to direct a portion of the bleaching beam to the photomultiplier tube (PMT) so that a small positive signal indicating the opening of the computer-controlled shutter was detected. Dichroic mirrors and cut-on filters were changed as needed for LIF detection with excitation at either 457.9 or 514.5 nm.

The remainder of the instrument was described in detail previously.[15] The modified instrument is illustrated in Fig. 1. Briefly, the 457.9 or 514.5 nm line from an Argon-ion (Ar^+) laser (Coherent Innova 90C-5; Santa Clara, CA) was split with a broadband cubic beamsplitter. The bleaching portion of the beam was directed through a computer-controlled shutter (Uniblitz 310 B; Vincent Associates, Rochester, NY), and focused through a fused-silica plano convex lens (f = 38 mm) onto the bore of the capillary at position F1. The detection portion of the beam was attenuated with neutral density filters (not shown). The detection beam was directed by a dichroic mirror (475DRLP for 457.9 nm or 540DRLP for 514.5 nm; Omega Optical; Brattleboro, VT) to a 20X microscope objective (0.4 NA) and focused on to the capillary bore at position F2. Fluorescence was collected at 180° and passed through two glass cut-on filters (LP-560-1.00 and CG-OG-550-1.00-2 for excitation at 514.5 nm or LP-475-1.00 and FCG-465-1.00 for excitation at 457.9 nm; CVI Laser Corporation, Albuquerque, NM) and spatially filtered (1.5 mm pinhole) prior to being detected with a PMT (Hamamatsu HC120; Bridgewater, NJ). The distance, d, between F1 and F2 (Fig. 1b) was determined daily using the method described previously.[15] The value of $d_{F1–F2}$ is:

$$d_{F1–F2} = \text{mean photobleached zone migration time} \times \frac{\text{injection end to F2 distance}}{\text{neutral marker migration time}} \quad (1)$$

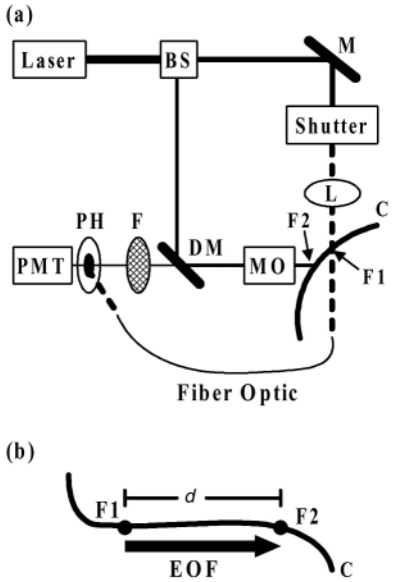

Fig. 1 (a) Schematic of the EOF monitoring instrument. BS, beamsplitter; M, mirror; L, plano-convex lens; C, capillary; F1, bleaching point on the capillary; F2, detection point on the capillary; MO, microscope objective; DM, dichroic mirror; F, long-pass filters; PH, pinhole; PMT, photomultiplier tube. (b) Enlarged view of the capillary indicating the position of the bleaching beam (F1) relative to the detection beam (F2) on the capillary. The distance between F1 and F2 is *d*.

2.3 Capillary electrophoresis

Fused silica capillary (50 μm id, 220 μm od) was obtained from SGE (Austin, TX) and used for all experiments. A Spellman CZE1000R high voltage power supply was used to apply the electrophoretic potential (Hauppauge, NY). The home-built CE instrument was described previously.[15] A Linear UVIS 204 detector (Linear Instruments, Reno, NV) with an on-column capillary cell was used for absorbance detection. The detection wavelength was 210 nm. The rise time for the absorbance detector was 1.0 s.

2.4 Instrument control and data acquisition

A program written in LabVIEW (National Instruments, Austin, TX) was used for data acquisition and instrument control. All data were acquired with a National Instruments PCI-6024E data acquisition board. All signals were filtered with a low-pass RC filter prior to acquisition. All data were analyzed with either Peak Fit 4.0 (SPSS Science, Chicago, IL) or Microsoft Excel (Microsoft Corp., Redmond, WA).

2.5 Fluorescence and absorbance spectra

Fluorescence excitation and emission spectra were obtained for 2.5×10^{-6} mol dm^{-3} rhodamine B in 5.0×10^{-2} mol dm^{-3} borate buffer (pH = 9.0) with a Model SQ-340 Aminco/Bowman Series 2 Luminescence Spectrometer (SLM Aminco, Urbana, IL). For the acquisition of the emission and excitation spectra, the excitation and emission monochromators were set at 552 and 577 nm, respectively. Absorbance spectra of the same solution of rhodamine B were obtained with a Model 8452A Diode Array Spectrophotometer (Hewlett Packard, Boise, ID).

2.6 Limit of detection (LOD) determination

The capillary was filled with 5.0×10^{-2} mol dm^{-3}, pH 9.0 borate buffer solution containing rhodamine B at concentrations from 1.0×10^{-5} to 7.0×10^{-9} mol dm^{-3}. At each rhodamine B concentration, a series of bleaching pulses were delivered to the running buffer at F1 as it flowed through the capillary. Signal was determined by measuring the difference between the fluorescence signal at each rhodamine B concentration with the shutter closed and the minimum value of the photobleached zone (negative peak) detected at F2. The LOD was defined as the concentration at which the signal was 3 times greater than the rms fluctuation of the fluorescence signal from unbleached rhodamine B. Conditions for the LOD study at 457.9 nm were based on the experimental conditions previously published.[15] The conditions for excitation at 457.9 nm were: bleaching power = 56 mW; detection power = 23 mW; bleaching pulse

duration = 250 ms; applied potential = 188 V cm^{-1}; data acquisition and filtering rates = 100 and 50 Hz, respectively; capillary length = 80 cm; length to detector = 70 cm. For excitation at 514.5 nm conditions were: bleaching power = 230 mW; detection power = 13 mW; bleaching pulse duration = 75 ms; applied potential = 138 V cm^{-1}; data acquisition and filtering rates = 150/50 Hz, respectively; capillary length = 80 cm; length to detector = 70 cm.

2.7 Bleaching pulse power and duration studies

The percentage of rhodamine B photobleached as a function of laser power was studied by exposing the fluorophore in the running buffer to 75 ms bleaching pulses. Experimental conditions were as follows: applied potential = 250 V cm^{-1}; running buffer = 5.0×10^{-2} mol dm^{-3} borate buffer (pH = 9.0) containing 4.0×10^{-8} mol dm^{-3} rhodamine B; flow rate = 0.200 cm s^{-1}; bleaching power = 29–232 mW; detection power = 14 mW; $d_{F1–F2}$ = 1.32 ± 0.01 mm; capillary length = 80 cm; length to detector = 70 cm; data acquisition and filtering rates = 150 and 50 Hz, respectively. The capillary was filled with blank borate buffer prior to each run and the fluorescence background in the absence of rhodamine B was measured. The baseline fluorescence signal was then determined by measuring the fluorescence due to the rhodamine B present in the running buffer with no photobleaching taking place (shutter closed). Then the computer-controlled shutter was allowed to open, exposing the rhodamine B in the running buffer to the bleaching beam. After the photobleaching event occurred at F1, the photobleached zone was detected as a negative peak at F2. The decrease in fluorescence due to photobleaching was measured at the minimum of the photobleached zone. The blank signal was subtracted from both the baseline fluorescence signal and the minimum value for the photobleached zone. The percentage of rhodamine B photobleached was determined by dividing the minimum value of the photobleached zone by the baseline fluorescence signal. Measurements were made for a series of 10 consecutive bleaching pulses (N = 10).

The effect of the bleaching pulse duration at F1 on the percent photobleaching observed at F2 was studied by varying the length of the bleaching pulse from 10 to 300 ms. Experimental conditions were as follows: bleaching power = 230 mW; detection power = 20 mW; running buffer = 5.0×10^{-2} mol dm^{-3} borate buffer (pH = 9.0) containing 4.0×10^{-8} mol dm^{-3} rhodamine B; applied potential = 188 V cm^{-1}; flow rate = 0.119 cm s^{-1}; $d_{F1–F2}$ = 0.709 ± 0.001 mm. The data were filtered at a rate 3 times (pulse width)$^{-1}$ and acquired at 10 times (pulse width)$^{-1}$ (*e.g.*, 10 Hz filtering and 33 Hz acquisition for a 300 ms pulse).

2.8 Characterization of the photobleached region as a function of flow rate and bleaching pulse duration

The capillary was filled with 5.0×10^{-2} mol dm^{-3} borate buffer (pH = 9.0) containing 4.0×10^{-8} mol dm^{-3} rhodamine B. The effect of flow rate on the photobleached region was examined using 75 ms bleaching pulses. The laser power was adjusted so that the bleaching power at F1 was 250 mW and the detection power at F2 was 12 mW. Data were filtered at 50 Hz and acquired at 150 Hz. The applied potential field was varied between 62.5 and 250 V cm^{-1}. The effect of bleaching pulse duration was examined by varying the duration of the bleaching pulses delivered at position F1 from 10 to 500 ms at each applied potential. Delay times between bleaching pulses were selected so that the negative peak observed at position F2 did not overlap with the start of the next bleaching pulse. The separation between F1 and F2 was $d_{F1–F2}$ = 0.635 mm.

2.9 Rhodamine B neutrality study

In order to confirm the neutrality of rhodamine B, samples of rhodamine B were coinjected electrokinetically with either mesityl oxide or DMSO (neutral markers) for 3 s at a potential of 235 V cm^{-1} and detected by absorbance. Replicate injections were conducted in both 5.0×10^{-2} mol dm^{-3} borate buffer (pH = 9.0) and 5.0×10^{-2} mol dm^{-3} bicarbonate buffer (pH = 8.35). The detection wavelength was 220 nm. The capillary used for these experiments was 85.0 cm long and 40.0 cm to the detector. All separations were carried out at 235 V cm^{-1}.

2.10 Phenolic acid separation

The UV/VIS absorbance detector was placed 40.0 cm from the injection end of the 85.0 cm capillary. The EOF monitoring instrument was located 75.0 cm from the injection end, after the absorbance detector. A solution containing syringic acid, 4-hydroxy-3-methoxybenzoic acid, *p*-hydroxycinnamic acid, 3,4-dihydroxybenzoic acid, 3,4-dihydroxycinnamic acid, and gallic acid was prepared in 1 + 1 (v/v) methanol–water. The capillary was first flushed with a 2.0 min electrokinetic injection (290 V cm^{-1}) of 0.1 mol dm^{-3} NaOH. The capillary was next flushed electrophoretically with 5.0×10^{-2} mol dm^{-3} sodium bicarbonate buffer (pH = 8.35) for 1 h.[21] The buffer was then replaced with 5.0×10^{-2} mol dm^{-3} sodium bicarbonate buffer (pH = 8.35) containing 4.00×10^{-7} mol dm^{-3} rhodamine B and was allowed to flush electrophoretically for 30 min prior to any sample injections. A single 3.0 s electrokinetic injection of the phenolic acid mixture was then made at an applied potential of 290 V cm^{-1}. The separation potential was 290 V cm^{-1}. EOF data were filtered at 300 Hz and acquired at 900 Hz.

3 Results and discussion

Our initial report of the photobleaching method for EOF monitoring demonstrated EOF measurement every 5.00 s throughout the course of a CE separation with a precision of 0.7% or better.[15] A neutral fluorophore is added to the running buffer at nanomolar concentrations. A computer-controlled shutter is opened briefly (10–500 ms in the work presented here), and a focused laser beam passes through the shutter, irradiating the dye-filled capillary at position F1 as indicated in Fig. 1. This creates a photobleached zone at F1, which flows to position F2 where it is detected by LIF as a negative peak. The measured flow rate is:

$$\text{flow rate} = \frac{d_{F1–F2}}{\Delta t_{F1–F2}} \quad (2)$$

where $d_{F1–F2}$ is the distance between positions F1 and F2 on the capillary and $\Delta t_{F1–F2}$ is the time required for the photobleached zone to migrate from F1 to F2. When the shutter is opened, a positive peak is observed at the LIF detector (F2) due to light from the bleaching beam at F1 that is delivered to the PMT by an optical fiber (Fig. 1a). This positive peak serves as a time stamp, indicating the time at which the shutter was opened and the photobleached zone was created at F1.[15]

3.1 Fluorophore concentration

The effect of the wavelength of light used for photobleaching and LIF detection was examined in order to decrease the concentration of neutral fluorophore required in the running buffer for EOF monitoring. Rhodamine B has been used as a neutral fluorophore here and in our previous work.[15] The excitation maximum for rhodamine B in 5.0×10^{-2} mol dm^{-3} borate buffer at pH 9.0 is 552 nm. In our previous work, an

irradiation wavelength of 457.9 nm was used.[15] The excitation spectrum of rhodamine B in borate buffer suggests that lower dye concentrations could be used with excitation by the 488.0 or 514.5 nm line from the Ar^+ laser used in this work. The absorbance of rhodamine B is 4 times greater at 488.0 nm and 10 times greater at 514.5 nm relative to 457.9 nm.

We compared the minimum rhodamine B concentrations required to monitor EOF using irradiation at 457.9 nm and 514.5 nm based on a S/N of 3. The minimum concentration for irradiation at 457.9 was 6×10^{-8} mol dm^{-3}, and the minimum concentration at 514.5 nm was 7×10^{-9} mol dm^{-3}. This improvement is expected based on the fluorescence excitation spectrum for rhodamine B. Differences in the bleaching power, pulse width and EOF rates between the experiments at 457.9 and 514.5 nm will also impact the detection limits obtained as discussed in the following sections. It is important to use low concentrations of neutral fluorescent buffer additive to minimize interference by the EOF monitoring method with a concurrent method of analyte detection such as UV/VIS absorbance. In our previous work, the concentration of rhodamine B was typically 4.00×10^{-7} mol dm^{-3}.[15] Irradiation at 514.5 nm was used for all other experiments presented here.

3.2 Distance between F1 and F2

As $d_{F1–F2}$ is decreased, the frequency at which the flow rate can be measured is increased. We have reduced $d_{F1–F2}$ to 0.635 mm, about an order of magnitude lower than in our previous work.[15] By decreasing $d_{F1–F2}$, the amount of time necessary for the photobleached zone created at F1 to reach the LIF detector at position F2 is reduced for a given flow rate. Previously, EOF was measured at a rate of 0.20 Hz ($d_{F1–F2}$ = 6.13 mm).[15] In the work presented here, we have measured EOF at frequencies of 0.7–1.0 Hz ($d_{F1–F2}$ = 0.635–1.33 mm). As examined in this paper, when $d_{F1–F2}$ is decreased, it becomes necessary to use shorter bleaching pulses and faster data acquisition in order to maintain the dynamic range and precision of EOF measurements obtained at greater values of $d_{F1–F2}$.

3.3 Rhodamine B photobleaching

Fig. 2 shows a plot of the percentage of rhodamine B photobleaching observed at F2 as the power of the bleaching pulses delivered at F1 is increased. The percentage of rhodamine B photobleached was determined by measuring the minimum fluorescence for the negative photobleached peak observed at F2 and dividing this value by the total fluorescence observed in the absence of bleaching (shutter closed). As expected, the percentage of rhodamine B photobleached increases with increasing laser power at F1.[19,20,22,23] As the power of the bleaching pulses increases, the percentage of rhodamine B photobleached begins to reach a plateau. The primary pathway for the photodegredation of rhodamine dyes is believed to take place from the excited triplet state.[23–27] The low quantum yield for formation of the excited triplet state of rhodamine B reduces the likelihood of complete photobleaching during a 75 ms exposure.[23,25,28]

Maximum photostability from a fluorophore is desired for sensitive LIF detection.[22,23] However, for flow monitoring based on photobleaching of a fluorophore[15,16] or optically gated injection of samples for CE,[19,20] it is desirable to use a fluorophore that is easily photobleached. Rhodamine B is photostable relative to many fluorescent dyes. For example, rhodamine B has a bleaching quantum efficiency of 0.5×10^{12} molecules photobleached W^{-1} s^{-1} cm^{-3}, which is 15 times smaller than that for fluorescein (7.4×10^{12} molecules photobleached W^{-1} s^{-1} cm^{-3}).[29] Fluorescein was not used because it is a charged species at the pH's used in these experiments. Due to the photostability of rhodamine B, high laser powers were used in order to achieve adequate photobleaching of rhodamine B.

Fig. 3 shows a plot of the percentage of rhodamine B photobleached as a function of the bleaching pulse duration. As expected, the percentage of rhodamine B photobleached increases as the duration of the bleaching pulse is increased.[16,20,22,23] When short bleaching pulses are applied, the percentage of rhodamine B photobleached (observed at F2) is determined by the total duration of exposure to the bleaching beam as well as diffusional broadening of the photobleached zone as it travels from position F1 to F2. As the bleaching pulse duration is increased, the amount of time that the fluorophore is exposed to the bleaching beam is lengthened, increasing the percentage of rhodamine B photobleached. Also, as the width of the bleached zone increases, the effect of diffusional broadening on the depth of the negative peak observed at F2 is reduced.

The plateau observed in the photobleaching efficiency of rhodamine B as a function of bleaching pulse duration occurs when two criteria are met: (1) the volume of flow during the time that the shutter is open exceeds the volume irradiated by the bleaching beam, and (2) the attenuation of the photobleached peak minimum due to diffusional broadening is negligible. Both of these criteria are flow rate dependent. As the flow rate increases, the volume flowing past F1 during a given

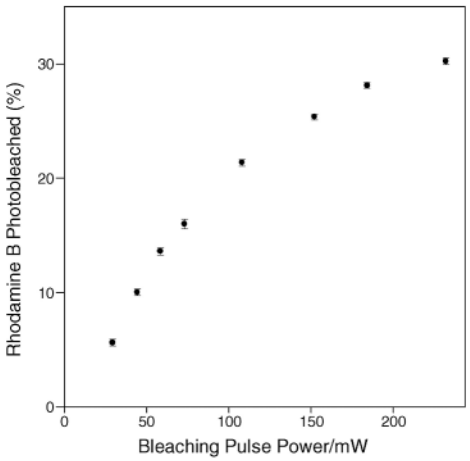

Fig. 2 Percent rhodamine B photobleached as detected at F2 *vs.* bleaching power at F1. Bleaching pulses (75 ms) were delivered to 4.0×10^{-8} mol dm^{-3} rhodamine B in 5.0×10^{-2} mol dm^{-3} borate buffer (pH = 9.0). (Flow rate = 0.200 cm s^{-1}; $d_{F1–F2}$ = 1.32 mm).

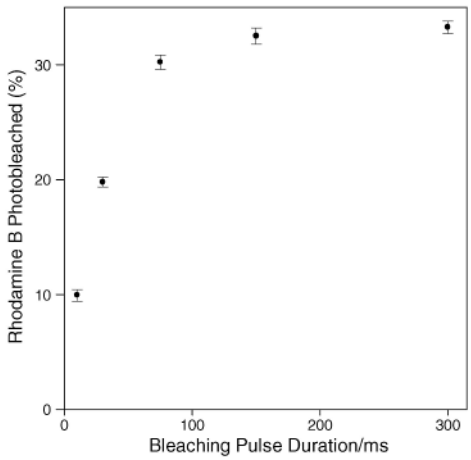

Fig. 3 Percent rhodamine B photobleached as detected at F2 *vs.* bleaching pulse duration (F1) for bleaching pulses delivered to 4.0×10^{-8} mol dm^{-3} rhodamine B in 5.0×10^{-2} mol dm^{-3} borate buffer (pH = 9.0). (Bleaching power = 230 mW; flow rate = 0.119 cm s^{-1}; $d_{F1–F2}$ = 0.709 mm).

period of time that the shutter is open will increase. This will decrease the bleaching pulse duration at which the percent photobleaching reaches a plateau. The effect of diffusional broadening will be reduced at higher flow rates, again reducing the bleaching pulse width at which a plateau is reached. The flow rate was 0.119 ± 0.001 cm s^{-1} ($\Delta t_{F1–F2}$ = 0.595 ± 0.002 s) for the data in Fig. 3, and the percent rhodamine B photobleached reaches 90% of its maximum value at ≃ 100 ms. As the flow rate decreases (at constant bleaching power and pulse duration), the percentage of rhodamine B photobleached will increase due to an increase in the amount of time that the fluorophore is exposed to the bleaching beam.[16,20,22,23]

3.4 Effect of bleaching pulse duration on photobleached zone width

A series of 10 to 500 ms bleaching pulses were delivered to a dye-filled capillary (4.0 × 10^{-8} mol dm^{-3} rhodamine B) at flow rates ranging from 0.0317 to 0.160 cm s^{-1}. These experiments were performed in order to observe the effects of flow rate and bleaching pulse duration on the photobleached zone as observed at F2. Data from this study are presented in Table 1 and Fig. 4. As expected, the width of the photobleached zone increases as the duration of the bleaching pulse is increased.

Fig. 4 illustrates what is observed at the extremes of bleaching pulse duration and flow rate used in this study. At a flow rate of 0.158 cm s^{-1} and $d_{F1–F2}$ of 0.635 mm, $\Delta t_{F1–F2}$ is 402 ± 4 ms, and the application of a 500 ms bleaching pulse is not completed before the leading edge of the photobleached zone reaches the LIF detector at F2 (Fig. 4a). Under identical conditions, a 10 ms bleaching pulse is well resolved from the photobleached zone (Fig. 4b). Fig. 4c shows the results for a 500 ms bleaching pulse at a flow rate of 0.0327 cm s^{-1}. Since $\Delta t_{F1–F2}$ is 1.94 ± 0.01 s, the photobleached zone is well resolved

Table 1 Photobleached zone width at fwhm for different values of EOF and bleaching pulse durations[a]

Bleaching pulse duration/ms	Photobleached zone width as a function of EOF/ms			
	0.160 cm s^{-1}	0.113 cm s^{-1}	0.0317 cm s^{-1}	Estimated dynamic range (1 Hz)[b]
10	34.9 ± 2.5	59.8 ± 4.5	—[c]	0.066–2.8 cm s^{-1}
30	47.5 ± 1.3	58.2 ± 2.1	276 ± 15	0.067–1.6 cm s^{-1}
100	96.0 ± 2.0	97.7 ± 2.3	291 ± 8	0.070–0.65 cm s^{-1}
200	204 ± 2	200 ± 3	353 ± 12	0.080–0.31 cm s^{-1}
500	—[d]	517 ± 3	518 ± 12	—[d]

[a] Bleaching pulse duration at F1 and photobleached zone width (fwhm) at F2 were determined for a $d_{F1–F2}$ of 0.635 mm with 4.0 × 10^{-8} mol dm^{-3} rhodamine B in 5.0 × 10^{-2} mol dm^{-3} borate buffer (pH = 9.0) with bleaching pulse and detection laser powers of 250 and 12 mW, respectively. Applied potentials were 250 V cm^{-1}, 187.5 V cm^{-1}, and 62.5 V cm^{-1} with average EOF rates of 0.160 cm s^{-1}, 0.113 cm s^{-1} and 0.0317 cm s^{-1}, respectively. (N = 10 consecutive bleaching pulses). [b] Values for the estimated dynamic range were calculated for an EOF sampling rate of 1 Hz. [c] A photobleached zone width could not be calculated due to poor S/N. [d] A photobleached zone width could not be calculated due to overlap of the bleaching pulse and the photobleached zone.

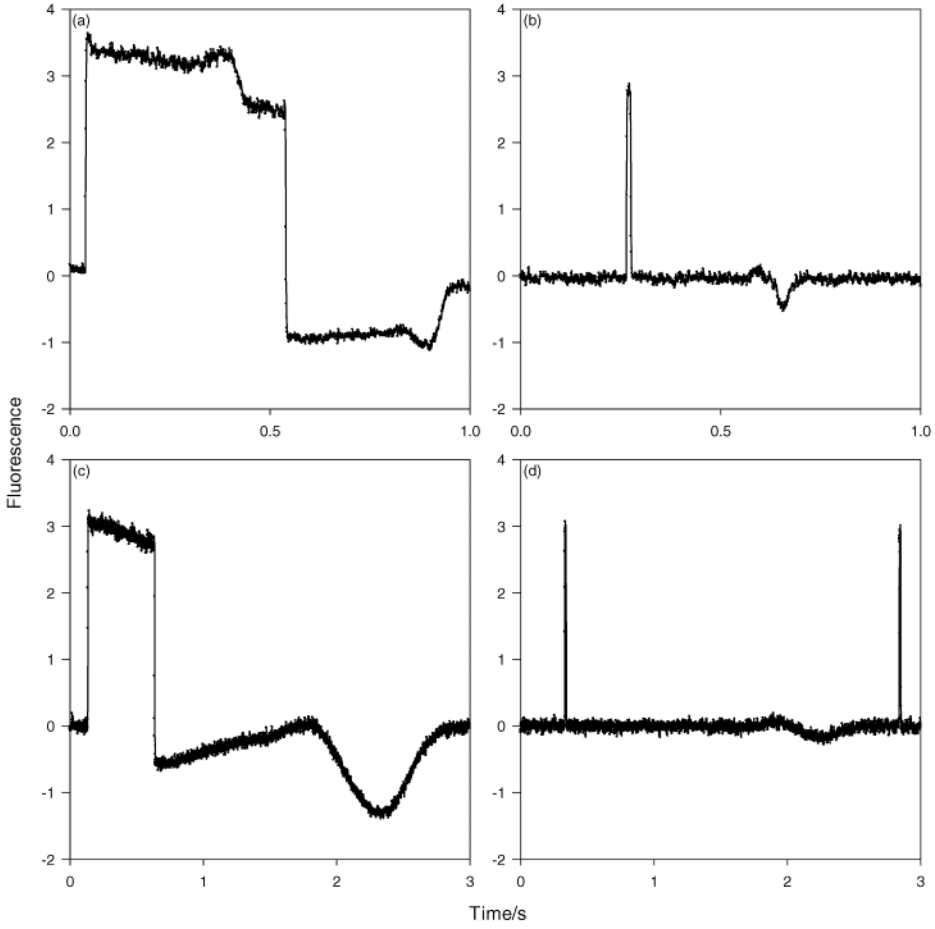

Fig. 4 (a) Electropherogram with a 500 ms bleaching pulse (positive peak) and the resulting decrease in fluorescence intensity (negative peak) at a flow rate of 0.158 cm s^{-1}. (b) Electropherogram for a 10 ms bleaching pulse at a flow rate of 0.158 cm s^{-1}. (c) Electropherogram for a 500 ms bleaching pulse at a flow rate of 0.0327 cm s^{-1}. (d) Electropherogram for a 10 ms bleaching pulse at a flow rate of 0.0327 cm s^{-1}. The second positive peak observed (d) is the beginning of the next EOF measurement. Experimental conditions are as listed in Table 1.

from the bleaching pulse. However, the photobleached zone for a 10 ms bleaching pulse (Fig. 4d) is barely perceptible due to diffusional broadening over 1.94 s. Table 1 includes an estimated dynamic range for flow measurements calculated for different bleaching pulse durations, a pulse repetition rate of 1 Hz and $d_{F1–F2}$ of 0.635 mm. In our previous work, a 250 ms pulse length was used with $d_{F1–F2}$ of 6.13 mm, resulting in a dynamic range for flow measurements of 0.10 to 2.4 cm s^{-1}.[15] Ideally, the distance between F1 and F2 would be as short as possible and the duration of the bleaching pulse would be infinitely short, thus allowing the rate at which EOF is monitored to be increased beyond 1 Hz with unlimited dynamic range.

Extremely narrow pulses provide the best dynamic range; however, the data in Figs. 3 and 4 illustrate that narrower bleaching pulses also result in decreased S/N for detection of the photobleached zone at F2 due to decreased bleaching and increased effects of diffusional broadening on the photobleached zone. Selection of a bleaching pulse width for an experiment is necessarily a compromise between pulse width and the minimum dye concentration required for adequate S/N. This compromise should include consideration of the desired measurement frequency and the range of flow rates expected for the experiment.

Inspection of the electropherograms from these experiments reveals an unexpected but reproducible feature that was unnoticed in earlier work.[15] This feature can be seen in Fig. 4 and is shown more clearly in Fig. 5. In Fig. 5a, a positive peak

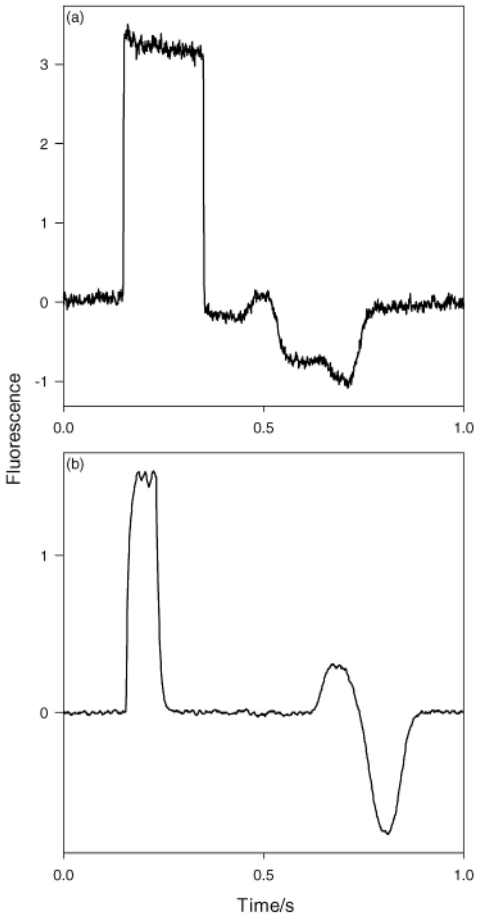

Fig. 5 Examples of photobleaching sequences with a positive peak overlapping with the photobleached zone. (a) Conditions are the same as those for Table 1. (Bleaching pulse duration = 200 ms; flow rate = 0.160 cm s^{-1}). (b) Capillary filled with 4.00 × 10^{-7} mol dm^{-3} rhodamine B in 5.0 × 10^{-2} mol dm^{-3} sodium bicarbonate buffer (pH = 8.35). (Bleaching power = 245 mW; detection power = 13 mW; flow rate = 0.211 cm s^{-1}, $d_{F1–F2}$ = 1.29 mm; bleaching pulse duration = 75 ms).

precedes and overlaps with the negative peak created by a 200 ms bleaching pulse (5.0 × 10^{-2} mol dm^{-3} borate buffer; pH = 9.0 with 4.0 × 10^{-8} mol dm^{-3} rhodamine B). The same phenomenon is shown in Fig. 5b for a 75 ms bleaching pulse (5.0 × 10^{-2} mol dm^{-3} sodium bicarbonate buffer; pH = 8.35 with 4.00 × 10^{-7} mol dm^{-3} rhodamine B), but diffusional broadening has obscured the stepped structure that is apparent in Fig. 5a. As discussed below the cause of this positive peak is not understood, but it is reproducible, and it is observed in nearly every experiment.

One hypothesis to explain these observations is that the positive peak is caused by changes in the refractive index of the solution due to heating during application of the photobleaching pulse.[17] This hypothesis requires rhodamine B to have a partial negative charge so that the photobleached zone separates from the heated solution zone as it travels from F1 to F2. We carefully reexamined the neutrality of rhodamine B to test this hypothesis, but these experiments give no indication that rhodamine B is negatively charged.

Other hypotheses have been considered but not tested experimentally. Rhodamine B fluorescence has been shown to decrease with increasing temperature in water, but this would lead to an effect opposite to our observations.[30] Several forms of rhodamine B are known to exist in aqueous solution, (neutral zwitterions, neutral lactones, cations and dimers), and the zwitterion is the expected form for the conditions used in this work.[30–35] A highly fluorescent cationic species would be consistent with our observations, but the cationic form of rhodamine B is present only at acidic pH's (pK_a = 3.1), and should be less fluorescent than the zwitterion with irradiation at 514 nm.[32,34,35]

The presence of this positive peak does not preclude making flow measurements using our method, but it must be considered when analyzing the data generated by this technique. In previous work, $\Delta t_{F1–F2}$ was measured from the half-maximum of the leading edge of the positive peak to the half-maximum of the leading edge of the negative peaks due to the photobleached zone.[15] The positive peak, overlapping with the photobleached zone will shift the apparent half-maximum of the leading edge of the negative peak and could shift the trailing edge of the negative peak depending on the extent of overlap. The calibration method used for our EOF measurements (section 2.2 and our previous publication)[15] will yield the same EOF rate regardless of whether the measurement is based on the leading or trailing edge of the peak. The only difference will be the calculated value for $d_{F1–F2}$. However, the precision of EOF measurement may differ depending on whether the leading or trailing edge is used for measurement. All data reported in this paper use the trailing edge for EOF measurement.

3.5 EOF measurement precision

In our previous work, the precision of our EOF measurements ranged from 0.2 to 0.7%.[15] For the data presented in this paper, the measured EOF precision ranges from 0.2 to 1.8%. The lower values for EOF measurement precision indicate that precision has not been sacrificed substantially by decreasing $d_{F1–F2}$, decreasing $\Delta t_{F1–F2}$ and increasing the measurement frequency. It is useful to consider the factors that affect EOF measurement precision using our method.

The first limitation to EOF measurement precision that must be considered is real fluctuations in EOF that occur on the time scale of our measurements. What this technique does is to repeatedly measure the EOF rate averaged over $\Delta t_{F1–F2}$ as the photobleached zone travels from F1 to F2. Values for $\Delta t_{F1–F2}$ in this work range from 0.393 to 1.94 s. For a value of $\Delta t_{F1–F2}$ of 393 ms, measured with a precision of 0.5%, the standard deviation of $\Delta t_{F1–F2}$ will be only 2.0 ms. It is not easy to determine whether the measurement precision is limited by the

technique or if it is limited by real fluctuations of EOF on the time scale of the measurement.

One factor that could lead to fluctuations in flow is variability in the voltage output from the electrophoresis power supply. The specifications for the power supply used in this work indicate an output noise of 0.1% peak-to-peak. This value is small relative to the observed precision of measured EOF. Current measurements during our experiments also indicate an RC time constant for the electrophoretic circuit on the order of 2 s.[36] Data presented later in this manuscript indicate that in some cases real fluctuations in EOF are determining the apparent measurement precision; however, it is unlikely that these are the result of fluctuations of the applied potential.

The time required for the shutter to close will impact the measurement precision. We measured the closing time of the shutter by directly observing the light from the bleaching beam detected at the PMT as indicated in Fig. 1. The shutter required 4 ± 1 ms to close ($N = 14$). The contribution of a 1 ms variation in the shutter opening to Δt_{F1-F2} measurement error is less than 0.3% for $\Delta t_{F1-F2} = 0.393$ s and 0.05% for $\Delta t_{F1-F2} = 1.94$ s.

Precision of EOF rate measurement is also affected by the rate at which the data is filtered and acquired. The data presented in Table 1 were filtered at 500 Hz and acquired at 1500 Hz. The contribution of the data filtering and acquisition rates is similar in magnitude to that of the shutter transfer time. As the data acquisition rate is increased, the possible precision of EOF measurements increases. Ideally, data would be acquired from all data channels at the maximum rate possible. However, the amount of data generated by acquiring multiple data channels at a high acquisition rate can be prohibitive. For example, a text file containing data acquired from 3 channels at 1500 Hz for 10 min is 17 MB in size. A compromise must be made between data acquisition rate and total acquisition time due to practical limitations of current computer resources.

The S/N for the photobleached zones detected will also impact the EOF measurement precision. If the S/N is too low, imprecise measured flow values will result. If S/N limits EOF measurement precision, this can be addressed by increasing the neutral dye concentration, increasing the bleaching power, or increasing fluorescence detection sensitivity.

The S/N for the photobleached zones is also affected by the EOF rate. As shown in Fig. 6, for a bleaching pulse of 75 ms, the S/N increases with increasing flow rate until a peak S/N value is reached near 0.1 cm s^{-1}. The S/N then decreases as the flow rate rises above 0.1 cm s^{-1}. As the flow rate drops below 0.1 cm s^{-1}, diffusion of the photobleached zone begins to decrease the S/N due to broadening of the photobleached zone prior to its detection at F2. As the flow rate increases above 0.1 cm s^{-1}, the percentage of rhodamine B photobleached decreases, and the S/N decreases accordingly. The decrease in S/N is due to a decrease in the effective exposure time of the rhodamine B to the bleaching beam at F1 as the flow rate increases.[16,20,22] This is further supported by the data in Fig. 3.

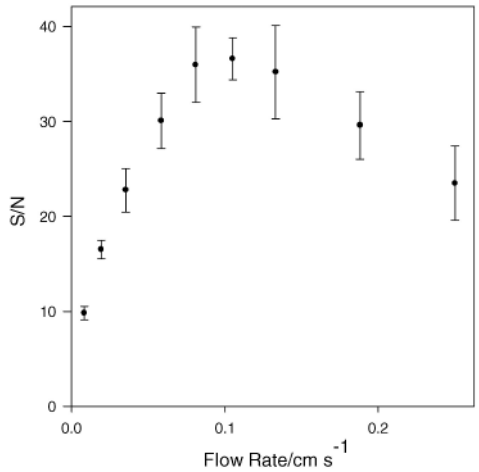

Fig. 6 S/N *vs.* flow rate for the detection of photobleached zones with a 75 ms bleaching pulse. All experiments were conducted with 4.0×10^{-8} mol dm^{-3} rhodamine B in 5.0×10^{-2} mol dm^{-3} borate buffer (pH = 9.0). (Bleaching power = 250 mW; detection power = 12 mW; $d_{F1-F2} = 0.747$ mm; data acquisition and filtering frequencies = 150 and 40 Hz, respectively).

The frequency at which the data is filtered and acquired will also affect the S/N. S/N can be improved by decreasing the frequency at which the input signal is filtered and acquired. However, as mentioned earlier in this section, the precision of the EOF measurement will be sacrificed.

3.6 Application of EOF monitoring to a separation with absorbance detection

One of the most common methods of detection used for CE is UV/VIS absorbance.[37] In order to demonstrate that our method of monitoring EOF does not interfere with concurrent methods of detection, a UV/VIS absorbance detector was used for analyte detection with EOF monitoring for a separation of six phenolic acids.[21] The UV/VIS absorbance detector was placed before the EOF detector (closer to the injection end) on the capillary. Bleaching pulses of 75 ms were used to measure EOF every 1.08 s. Data were filtered at 300 Hz and acquired at 900 Hz. In order to ensure a high S/N for flow measurements, the concentration of rhodamine B added to the CE running buffer was 4.00×10^{-7} mol dm^{-3}. The separation and detection conditions (detection wavelength = 210 nm) were based on a published separation of phenolic acids by Cartoni and co-workers.[21]

Fig. 7a shows the elution of the phenolic acids as well as a peak from the methanol–water mixture as detected at the UV/VIS detector 40.0 cm from the injection end of the capillary. Fig. 7b shows a plot of EOF rate values as measured 80.0 cm from the injection end of the capillary. The separation was also carried out on the same instrument using only UV/VIS detection without rhodamine B added to the running buffer (data not shown). The separation and baseline obtained with the rhodamine B present in the running buffer is indistinguishable from the control experiment without rhodamine B, and our results are almost identical to the published separation.[21] Clearly, monitoring EOF using our method is not influencing the separation and analyte detection by UV/VIS absorbance.

The average EOF rate over the entire experiment was determined to be 0.211 cm s^{-1} as measured with the methanol–water neutral peak at 202 s. When the flow rates measured by our EOF monitoring technique over the course of the separation are plotted (Fig. 7b), it can be seen that the flow actually fluctuates between 0.200 to 0.222 cm s^{-1} with an average flow rate of 0.211 ± 0.003 cm s^{-1} (RSD = 1.6%; $N = 482$) measured over 545 s. The overall average flow rate measured by our technique until the neutral marker elutes past the UV/VIS absorbance detector at 202 s is 0.211 ± 0.002 cm s^{-1}. From 203 to 556 s, our technique measures a flow rate of 0.211 ± 0.003 cm s^{-1}. In this case, the overall flow rate is indistinguishable before and after the neutral marker elutes past the UV/VIS absorbance detector. However, in cases where the EOF is less stable over long periods of time, only our method is capable of observing a difference.

In order to determine whether fluctuations in EOF were due to instabilities in the EOF from interactions between the sample and the capillary, EOF was monitored for approximately 20 s when no sample had been injected into the capillary. A precision of 1.0% ($N = 19$ consecutive bleaching pulses) was observed for the EOF without sample injection. This precision measured

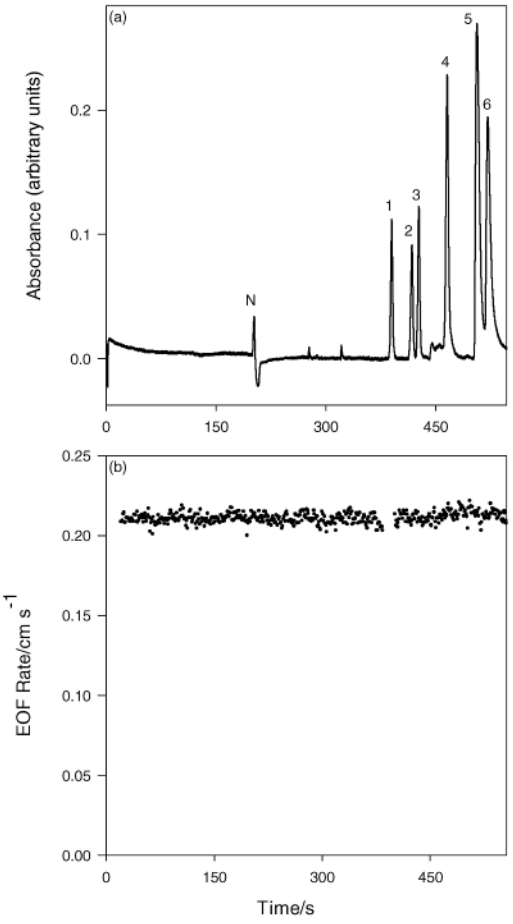

Fig. 7 Separation of phenolic acids with simultaneous EOF monitoring. (a) Electropherogram of a separation of 6 phenolic acids (detection λ = 210 nm). Peaks are identified as (N) methanol–water, (1) syringic acid (3.8×10^{-4} mol dm^{-3}), (2) *p*-hydroxycinnamic acid (4.9×10^{-4} mol dm^{-3}), (3) 4-hydroxy-3-methoxybenzoic acid (4.1×10^{-4} mol dm^{-3}), (4) 3,4-dihydroxycinnamic acid (1.5×10^{-3} mol dm^{-3}), (5) 3,4-dihydroxybenzoic acid (1.4×10^{-3} mol dm^{-3}) and (6) gallic acid (3.0×10^{-3} mol dm^{-3}). (b) EOF rate *vs.* time for EOF monitoring performed during the phenolic acid separation. The capillary was filled with 4.00×10^{-7} mol dm^{-3} rhodamine B in 5.0×10^{-2} mol dm^{-3} sodium bicarbonate buffer (pH = 8.35). The sample was electrokinetically injected for 3.0 s at an applied potential of 290 V cm^{-1}. (Bleaching power = 245 mW; detection power = 13 mW; bleaching pulse duration = 75 ms; average flow rate = 0.211 cm s^{-1}; d_{F1-F2} = 1.29 mm).

in the absence of sample indicates that the 1.6% precision in EOF observed during the separation of the phenolic acids is affected by the presence of the sample. The nature of these fluctuations due to sample injection is not yet understood and is under investigation.

Acknowledgements

The authors would like to thank Joseph Batts for his contributions to this work. This research was supported by startup funds from the University of Tennessee. K.F.S. was supported by the National Science Foundation RSEC Program at UT (9974734).

References

1 T. Wielgos, P. Turner and K. Havel, *J. Capillary Electrophor.*, 1997, **4**, 273.
2 G. Guiochon, *Am. Lab.*, 1998, **30**, 14.
3 J. P. Schaeper and M. J. Sepaniak, *Electrophoresis*, 2000, **21**, 1421.
4 S. Terabe, K. Otsuka, K. Ichikawa, A. Tsuchiya and T. Ando, *Anal. Chem.*, 1984, **56**, 111.
5 K. D. Lukacs and J. W. Jorgenson, *J. High Resolut. Chromatogr. Chromatogr. Commun.*, 1985, **8**, 407.
6 A. A. A. M. VanDeGoor, B. J. Wanders and F. M. Everaerts, *J. Chromatogr.*, 1989, **470**, 95.
7 J. A. Taylor and E. S. Yeung, *Anal. Chem.*, 1993, **65**, 2928.
8 T. Tsuda, M. Ikedo, G. Jones, R. Dadoo and R. N. Zare, *J. Chromatogr.*, 1993, **632**, 201.
9 T. T. Lee, R. Dadoo and R. N. Zare, *Anal. Chem.*, 1994, **66**, 2694.
10 J. Preisler and E. S. Yeung, *Anal. Chem.*, 1996, **68**, 2885.
11 T. Tsuda, S. Kitagawa, R. Dadoo and R. N. Zare, *Bunseki Kagaku*, 1997, **46**, 409.
12 P. H. Paul, M. G. Garguilo and D. J. Rakestraw, *Anal. Chem.*, 1998, **70**, 2459.
13 A. E. Herr, J. I. Molho, J. G. Santiago, M. G. Mungal, T. W. Kenny and M. G. Garguilo, *Anal. Chem.*, 2000, **72**, 1053.
14 U. Tallarek, E. Rapp, T. Scheenen, E. Bayer and H. V. As, *Anal. Chem.*, 2000, **72**, 2292.
15 K. F. Schrum, J. M. Lancaster, S. E. Johnston and S. D. Gilman, *Anal. Chem.*, 2000, **72**, 4317.
16 J. H. Sugarman and R. K. Prud'homme, *Ind. Eng. Chem. Res.*, 1987, **26**, 1449.
17 J. C. StClaire and M. A. Hayes, *Anal. Chem.*, 2000, **72**, 4726.
18 R. T. Kennedy, I. German, J. E. Thompson and S. R. Witowski, *Chem. Rev.*, 1999, **99**, 3081.
19 C. A. Monnig and J. W. Jorgenson, *Anal. Chem.*, 1991, **63**, 802.
20 L. Tao, J. E. Thompson and R. T. Kennedy, *Anal. Chem.*, 1998, **70**, 4015.
21 G. Cartoni, F. Coccioli and R. Jasionowska, *J. Chromatogr., A*, 1995, **709**, 209.
22 R. A. Mathies, K. Peck and L. Stryer, *Anal. Chem.*, 1990, **62**, 1786.
23 C. Eggeling, J. Widengren, R. Rigler and C. A. M. Seidel, *Anal. Chem.*, 1998, **70**, 2651.
24 M. Yamashita and H. Kashiwagi, *IEEE J. Quantum Electron.*, 1976, **QE-12**, 90.
25 V. E. Korobov and A. K. Chibisov, *J. Photochem.*, 1978, **9**, 411.
26 G. Jones, in *Dye Laser Principles with Applications*, ed. F. J. Duarte and L. W. Hillman, Academic Press, Inc., Boston, 1990, pp. 287.
27 S. Becker, I. Gregor and E. Thiel, *Chem. Phys. Lett.*, 1998, **283**, 350.
28 M. Yamashita, A. Kuniyasu and H. Kashiwagi, *J. Chem. Phys.*, 1977, **66**, 986.
29 D. Beer and J. Weber, *Opt. Commun.*, 1972, **5**, 307.
30 D. A. Hinckley, P. G. Seybold and D. P. Borris, *Spectrochim. Acta*, 1986, **42A**, 747.
31 J. E. Selwyn and J. I. Steinfeld, *J. Phys. Chem.*, 1972, **76**, 762.
32 I. L. Arbeloa and P. R. Ojeda, *Chem. Phys. Lett.*, 1981, **79**, 347.
33 D. A. Hinckley and P. G. Seybold, *Spectrochim. Acta, Part A*, 1988, **44A**, 1053.
34 F. L. Arbeloa, P. R. Ojeda and I. L. Arbeloa, *J. Lumin.*, 1989, **44**, 105.
35 F. L. Arbeloa, T. L. Arbeloa, M. J. T. Estevez and I. L. Arbeloa, *J. Phys. Chem.*, 1991, **95**, 2203.
36 X. Huang, W. F. Coleman and R. N. Zare, *J. Chromatogr.*, 1989, **480**, 95.
37 R. Weinberger, *Practical Capillary Electrophoresis*, Academic Press, San Diego, 2nd edn., 2000.